

Fig. 2. (a) Schematic coronal brain sections showing the location of AC nerve-activated, second-order vestibular neurons. Sections through the superior (S), lateral (L), descending (D), and medial (M) vestibular nuclei are arranged rostrocaudally (1–8). Neurons are represented by separate symbols according to the axonal pathway and the most caudal level of effective stimulation. Circle, VS neuron; triangle, VOS neuron; square, VO neuron. Open triangle and square, vestibulosplinal neurons that were activated antidromically only from the cervical segments; closed symbols, vestibulosplinal neurons that were activated antidromically from the T1 segment and not from the L3 segment. Neurons that could not be identified are not shown. (b) A schematic horizontal brain section showing the location of AC nerve-activated, second-order vestibular neurons. Open circles, vestibulosplinal neurons that were activated antidromically only from the cervical segments; closed symbols, vestibulosplinal neurons that were activated antidromically from the T1 segment but not from the L3 segment.

i-LVST, MVST, and c-LVST to antidromically activate vestibular neurons, we demonstrated that AC nerve-activated vestibulosplinal neurons send axons to the spinal cord through these three descending tracts. The majority of them projected axons to cervical segments, while the remaining neurons projected to thoracic or lumbar levels. The majority of the neurons projected through the MVST.

The projection levels within the spinal cord and the main descending pathway of vestibulosplinal neurons characterized in the present study are consistent with those reported in previous studies: neurons that send descending axons through the MVST mainly project to the upper cervical segments [7,8,13]. The properties of the neurons we studied are also consistent with those described in previous studies, where it was shown that AC nerve stimulation evokes disynaptic PSPs in bilateral neck extensor and flexor motoneurons via vestibulosplinal neurons. More specifically, neurons synaptically connected to the i-extensor motoneurons project through the i-LVST, and neurons synaptically connected to the c-extensor and bilateral flexor motoneurons project through the MVST [2,14,15,20–22,25,26]. A small portion of MVST neurons and few i-LVST neurons projected to the thoracic or lumbar segments. Since in previous studies we found no definitive electrophysiological evidence of synaptic potentials in forelimb motoneurons in the cat after stimulating the AC nerve [20,21], projections from the AC nerve to forelimb motoneurons might be weak.

The present study clearly demonstrated that AC nerve-activated vestibulosplinal neurons send axons through the c-LVST to the cervical spinal cord, but not to the thoracic or lumbar levels. Most of these neurons were VOS neurons. The present finding suggests that AC nerve-activated c-LVST neurons also exert influence on the spinal neurons or neural circuits. Considering that all of these project to the upper cervical segments, and that most of them are VOS neurons, possible targets of c-LVST neurons may be the oculomotor and the c-neck motoneurons; these may be closely related to the control of combined eye-head movements [19]. In this regard, it has already been shown that there exist AC nerve-activated VOS neurons that have axons traversing the c-MVST and connecting to contralateral neck motoneurons [19]. Functional differences between the c-LVST neurons and the c-MVST neurons need to be clarified in a future study. On the other hand, HC nerve-activated vestibulosplinal neurons have been shown to lack a projection through the c-LVST [16]. Whether posterior canal nerve-activated and otolith-activated vestibulosplinal neurons project axons through the c-LVST also remains to be clarified.

Tendencies that the majority of vestibulosplinal neurons project axons to the cervical segments through the MVST were also observed in HC nerve-activated [16] and SAC nerve-activated [13] vestibulosplinal neurons. An exception to this tendency is the projection patterns of UT nerve-activated vestibulosplinal neurons [12]: the proportion of these neurons that projects axons to the cervical segments through the MVST were lower than in the AC nerve-, HC nerve-, and SAC nerve-activated vestibulosplinal neurons. In addition, while few AC nerve-, HC nerve-, and SAC nerve-activated vestibulosplinal neurons sent axons to the lumbar cord, many more (more than twice as

many) UT nerve-activated vestibulospinal neurons projected to the lumbar segment, and all of these sent their axons through the i-LVST. While UT nerve-activated vestibulospinal neurons appear to contribute to the control of muscles in the lower half of the body, as well as to the control of neck muscles, AC nerve-activated vestibulospinal neurons and HC nerve- and SAC nerve-activated vestibulospinal neurons may primarily target the neck muscles, and thus contribute to the vestibulocollic reflex.

Acknowledgements

This study was supported by a research grant from the Japan Space Forum promoted by NASDA (National Space Development Agency of Japan).

References

- [1] T. Akaike, V.V. Fanardjian, M. Ito, M. Kumada, H. Nakajima, Electrophysiological analysis of the vestibulospinal reflex pathway of rabbit. I. Classification of tract cells, *Exp. Brain Res.* 17 (1973) 477–496.
- [2] K. Fukushima, B. Peterson, V.J. Wilson, Vestibulospinal, reticulospinal and interstitiospinal pathways in the cat, *Prog. Brain Res.* 50 (1979) 121–136.
- [3] W. Graf, K. Ezure, Morphology of vertical canal related second order vestibular neurons in the cat, *Exp. Brain Res.* 63 (1986) 35–48.
- [4] W. Graf, R.A. McCrea, R. Baker, Morphology of posterior canal related secondary vestibular neurons in rabbit and cat, *Exp. Brain Res.* 52 (1983) 125–138.
- [5] N. Isu, J. Yokota, Morphological study on the divergent projection of axon collaterals of medial vestibular nucleus neurons in the cat, *Exp. Brain Res.* 53 (1983) 151–162.
- [6] R. Nyberg-Hansen, T.A. Mascitti, Sites and mode of termination of fibers of the vestibulospinal tract in the cat. An experimental study with silver impregnation methods, *J. Comp. Neurol.* 122 (1964) 369–388.
- [7] J.M. Petras, Cortical, tectal and tegmental fiber connections in the spinal cord of the cat, *Brain Res.* 6 (1967) 275–324.
- [8] W. Precht, H. Shimazu, Functional connections of tonic and kinetic vestibular neurons with primary vestibular afferents, *J. Neurophysiol.* 28 (1965) 1014–1028.
- [9] S. Rapoport, A. Susswein, Y. Uchino, V.J. Wilson, Properties of vestibular neurons projecting to neck segments of the cat spinal cord, *J. Physiol. (Lond.)* 268 (1977) 493–510.
- [10] P.K. Rose, E.V. S. Norkum, M. Neuber-Hess, Projections from the lateral vestibular nucleus to the upper cervical spinal cord of the cat: a correlative light and electron microscopic study of axon terminals stained with PHA-L., *J. Comp. Neurol.* 410 (1999) 571–585.
- [11] H. Sato, K. Endo, H. Ikegami, M. Imagawa, M. Sasaki, Y. Uchino, Properties of utricular nerve-activated vestibulospinal neurons in cats, *Exp. Brain Res.* 112 (1996) 197–202.
- [12] H. Sato, M. Imagawa, N. Isu, Y. Uchino, Properties of saccular nerve-activated vestibulospinal neurons in cats, *Exp. Brain Res.* 116 (1997) 381–388.
- [13] Y. Shinoda, Y. Sugiuchi, T. Futami, N. Ando, T. Kawasaki, Inputs patterns and pathways from the six semicircular canals to motoneurons of neck muscles. I. The multifidus muscle group, *J. Neurophysiol.* 72 (1994) 2691–2702.
- [14] Y. Shinoda, Y. Sugiuchi, T. Futami, N. Ando, J. Yagi, Inputs patterns and pathways from the six semicircular canals to motoneurons of neck muscles. II. The longissimus and semispinalis muscle groups, *J. Neurophysiol.* 77 (1997) 1234–1258.
- [15] A. Sugita, R. Bai, M. Imawaga, H. Sato, M. Sasaki, N. Kitajima, I. Koizuka, Y. Uchino, Properties of horizontal semicircular canal nerve-activated vestibulospinal neurons in cats, *Exp. Brain Res.* 156 (2004) 478–486.
- [16] Y. Sugiuchi, Y. Izawa, Y. Shinoda, Trisynaptic inhibition from the contralateral vertical semicircular canal nerves to neck motoneurons mediated by spinal commissural neurons, *J. Neurophysiol.* 73 (1995) 1973–1987.
- [17] J.I. Suzuki, K. Goto, K. Tokumatsu, B. Cohen, Implantation of electrodes near individual vestibular nerve branches in mammals, *Ann. Otol. Rhinol. Laryngol.* 78 (1969) 815–826.
- [18] Y. Uchino, N. Hirai, Axon collaterals of anterior semicircular canal-activated vestibular neurons and their coactivation of extraocular and neck motoneurons in the cat, *Neurosci. Res.* 1 (1984) 309–325.
- [19] Y. Uchino, N. Isu, T. Ichikawa, S. Sastoh, S. Watanabe, Properties and localization of the anterior semicircular canal-activated vestibulocollic neurons in the cat, *Exp. Brain Res.* 71 (1988) 345–352.
- [20] Y. Uchino, N. Isu, A. Sakuma, T. Ichikawa, K. Hiranuma, Axonal trajectories of inhibitory vestibulocollic neurons activated by the anterior semicircular canal nerve and their synaptic effects on neck motoneurons in the cat, *Exp. Brain Res.* 82 (1990) 14–24.
- [21] Y. Uchino, S.-I. Sasaki, M. Imagawa, H. Uchino, N. Isu, A. Sakuma, Properties and axonal trajectories of inhibitory vestibulocollic neurons in the horizontal canal system of the cat, *Neurosci. Res. Suppl.* 11 (1990) S139.
- [22] Y. Uchino, H. Sato, M. Sasaki, M. Imagawa, H. Ikegami, N. Isu, W. Graf, Sacculocollic reflex arcs in cats, *J. Neurophysiol.* 77 (1997) 3003–3012.
- [23] V.J. Wilson, L.P. Fempel, Specificity of semicircular canal input to neurons in the pigeon vestibular nuclei, *J. Neurophysiol.* 35 (1972) 253–264.
- [24] V.J. Wilson, M. Maeda, Connections between semicircular canals and neck motoneurons in the cat, *J. Neurophysiol.* 37 (1974) 357–364.
- [25] V.J. Wilson, J.G. Melvill, The vestibulospinal system, in: *Mammalian Vestibular Physiology*, Plenum Press, New York, London, 1979, pp. 185–248.

Model experiments of BPPV using isolated utricle and posterior semicircular canal

Taro Inagaki*, Mamoru Suzuki, Koji Otsuka, Naoharu Kitajima,
Masayoshi Furuya, Yasuo Ogawa, Tsuyoshi Takenouchi

Department of Otolaryngology, Tokyo Medical University, 6-7-1 Nishishinjuku, Shinjuku-ku, Tokyo 160-0023, Japan

Received 14 June 2005; accepted 16 September 2005

Available online 23 November 2005

Abstract

Objectives: This study was aimed to experimentally investigate the effect of returned otoconia on the utricular using isolated utricles. The effect of interposed otoconia in models of canalolithiasis and cupulolithiasis were also investigated using isolated posterior semicircular canal (PSC).

Methods: Bullfrogs were used. The utricles (Experiment I) and PSC (Experiment II) were removed in Ringer solution. Experiment I-a: The otoconia were carefully removed from the utricular macula with gentle flush of Ringer solution. Before and after the otoconial removal, sinusoidal rotatory stimulation (0.1 Hz, 135°) was given to record utricular compound action potentials (CAPs). Experiment I-b: (1) Instantaneous changes in the utricular potentials when the otoconial mass was positioned on the macula were recorded. (2) Utricular CAP changes in response to sinusoidal rotation immediately and 10 min after the otoconial positioning were recorded. Experiment II: PSC CAPs due to sinusoidal rotatory stimulation in normal specimen, canalolithiasis and cupulolithiasis models were recorded.

Results: Experiment I-a: The utricular CAPs in response to sinusoidal rotation showed sinusoidal oscillation. However, this oscillation disappeared after the otoconial removal. Experiment I-b: (1) The utricular potentials transiently increased for 3–4 s after positioning the otoconial mass. (2) The utricular CAPs increased in seven specimens and decreased in four. Ten minutes after the CAPs were almost the same as immediately after otoconial positioning. Experiment II: In cupulolithiasis model, the PSC CAPs decreased in all specimens.

Conclusions: The otoconia played an essential role as a transducer of acceleration to the utricular macula. Otoconia returned to the utricular macula change utricular reactivity and hence are the possible cause of dizziness after physical therapy. PSC responses to sinusoidal rotation were suppressed in cupulolithiasis model.

© 2005 Elsevier Ireland Ltd. All rights reserved.

Keywords: BPPV; Frog utricle; Frog semicircular canal; Canalolithiasis; Cupulolithiasis

1. Introduction

Benign paroxysmal positional vertigo (BPPV) is a common vertigo with favorable prognosis. It basically remits spontaneously, but some cases are intractable and persist for several years. Canalolithiasis [1] of the posterior semicircular canal (PSC) is now considered to be a principal pathology.

A variety of physical therapy have been performed based on the canalolithiasis theory. Nevertheless, mild vertigo or

dizziness occasionally persists for several days after physical therapy. It is suspected that the otoconia returned from semicircular canal into the utricle are responsible for this symptom. Caloric response and vestibulo-ocular reflex (VOR) sometimes reduce in lateral semicircular canal type BPPV. It is suggested that the otoconia interposed within the lateral semicircular canal are responsible for this phenomena.

In the present study, we prepared a model of BPPV using an isolated utricle to investigate the effect of returned otoconia on the utricular macula. We also prepared models of canalolithiasis and cupulolithiasis using isolated PSC to investigate the physiological effect of the interposed otoconia in both models.

* Corresponding author. Tel.: +81 3 3342 6111x5787;

fax: +81 3 3346 9275.

E-mail address: QUE07470@nifty.com (T. Inagaki).

2. Materials and methods

2.1. Experiment I: effect of returned otoconia on the utricular potentials

Bullfrogs (*Rana catesbeiana*) weighing 110–220 g were used. After deep anesthesia with ether they were decapitated, following the ethical rules of the animal experiment in Tokyo Medical University. Under a dissection microscope the anterior and lateral semicircular canals and utricle were removed together with the superior vestibular nerve in Ringer solution according to the method of Suzuki et al. [2]. The anterior and lateral ampullary nerves were transected at the site of insertion into the ampullae in order to eliminate their influence on the utricle. The membrane around the utricular macula was removed to allow direct vision of the macula. The specimen was fixed with fine glass needles 3 cm from the center of a glass dish filled with Ringer solution. The ampullae were placed outward and the utricle inward. The vertical line to the tangential line at the striola center was toward the center of the dish. Care was taken to ensure the utricular macula being in a horizontal plane (Fig. 1).

The glass dish was magnetically fixed to the center of a 30 cm-diameter turn table. The turn table was sinusoidally rotated by a computer-controlled motor. The rotation cycle

was set 0.1 Hz, the rotation angle 135°, and the maximum angular velocity 84° s⁻¹. The superior vestibular nerve was sucked into the glass suction electrode to record utricular compound action potentials (CAPs).

2.1.1. Experiment I-a

First, role of the otoconia for effectively stimulating the sensory epithelium was examined. The otoconia were carefully removed from the utricular macula with gentle flush of Ringer solution. Utricular CAPs in response to sinusoidal rotatory stimulus were recorded before and after the otoconial removal.

2.1.2. Experiment I-b

Changes in utricular potentials were examined before and after positioning the otoconial mass on the macula. The otoconia of the ipsilateral saccular macula were used for positioning.

- (1) Instantaneous changes in the utricular potentials when the otoconial mass was positioned on the macula were recorded without sinusoidal rotation (two specimens).
- (2) Changes in the utricular CAPs immediately and 10 min after the otoconial mass positioning were recorded with sinusoidal rotation (11 specimens).

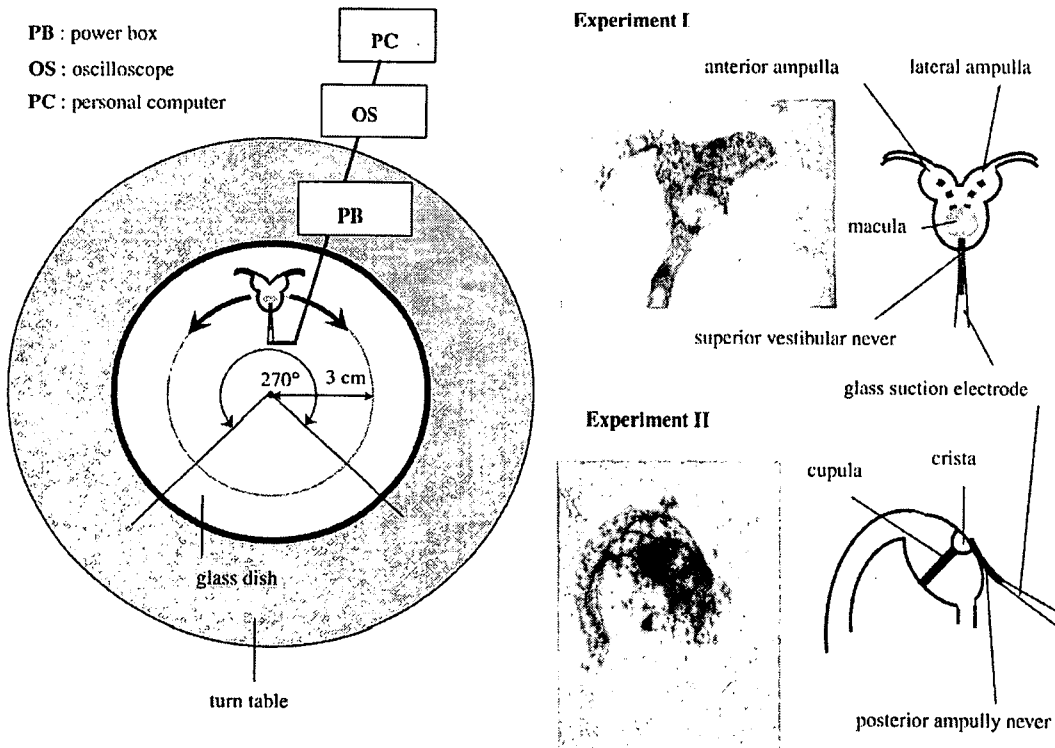


Fig. 1. Schema of experimental setting. A specimen set in a glass dish on a turn table (left). Details of preparation in Experiments I and II are shown together with photomicrographs (right).

2.2. Experiment II: effect of the otoconia on PSC CAPs in canalolithiasis and cupulolithiasis models

After deep anesthesia with ether, the bull frogs were decapitated. The PSC and the ampullary nerve were removed according to the method of Suzuki et al. [3]. The specimen was placed in a glass dish with the ampulla toward the right side and the nerve toward the outside (Fig. 1). The cupula top and the crista were on the line toward the rotation center. The same sinusoidal rotation was applied as in Experiment I. The PSC ampullary nerve was sucked into the glass suction electrode to record PSC CAPs.

Eight canalolithiasis and eight cupulolithiasis models were prepared according to the method of Suzuki et al. [4].

We first recorded the CAPs of normal specimens and then recorded the CAPs after creating either the canalolithiasis model or the cupulolithiasis model.

The utricular CAPs (Experiment I) or the PSC CAPs (Experiment II) were converted into spike density histograms (Fig. 1). The differences between the maximum and the minimum spike density in three consecutive recordings were averaged and were designated as the response intensity (Fig. 2).

3. Results

3.1. Experiment I-a

The utricular CAP in response to sinusoidal rotatory stimulation showed sinusoidal oscillation. However, this oscillation was no longer seen when the otoconia were removed. The spontaneous discharges did not change (Fig. 3).

3.2. Experiment I-b

(1) The utricular potentials transiently increased for 3–4 s after positioning the otoconial mass. The maximum spike count approximately doubled. A similar response

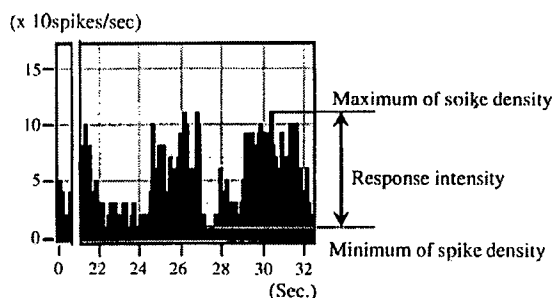


Fig. 2. Measurement of CAP response intensity. Differences between the maximum and the minimum values were averaged and designated as response intensity.

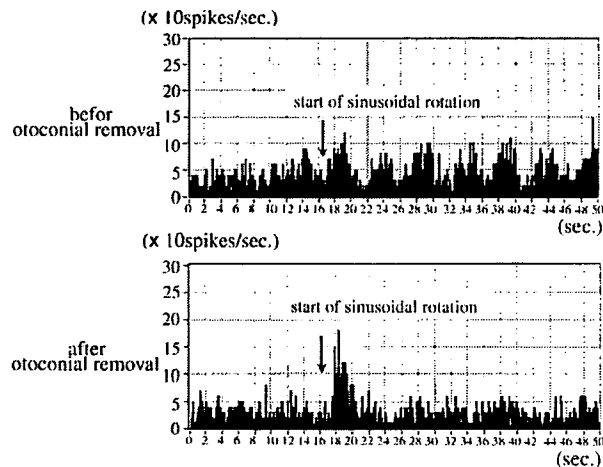


Fig. 3. Effect of otoconial removal on the utricular CAP (Experiment I-a). The histograms before the otoconial removal showed sinusoidal oscillation associated with sinusoidal rotation (upper recording). The oscillation disappeared after otoconial removal (lower recording).

was observed when the otoconia were repositioned 30 s later (Fig. 4).

(2) The histograms of utricular CAP in response to sinusoidal rotation showed sinusoidal oscillation of 0.2 Hz, and the averaged difference between the maximum and minimum (response intensity) before positioning the otoconial mass was 114.2 spikes/s. Immediately after the positioning the otoconial mass the response intensity ranged from 98.4 spikes/s to 146.6 spikes/s. In seven specimens it increased, and in four decreased. Ten minutes after the positioning it ranged from 103.3 spikes/s to 141.7 spikes/s, and was almost the same as immediately after the otoconial positioning (Fig. 5). Changes in the response intensity were expressed in percentage with the prepositioning value as 100% (graph in Fig. 5).

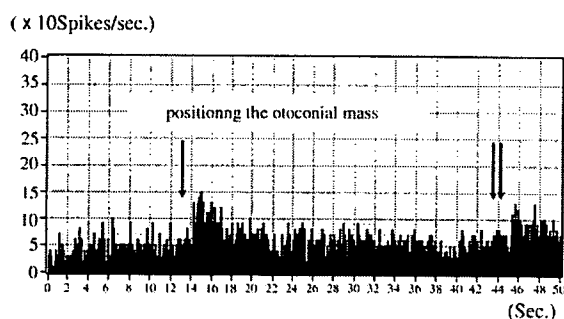


Fig. 4. Effect of otoconial positioning on the utricle without sinusoidal rotation (Experiment I-b (1)). Utricular potentials transiently increased for 3–4 s immediately after the otoconial mass was positioned (arrow) on the macula. The spike count approximately doubled. A similar response was observed when the otoconial mass was repositioned about 30 s later (double arrows).

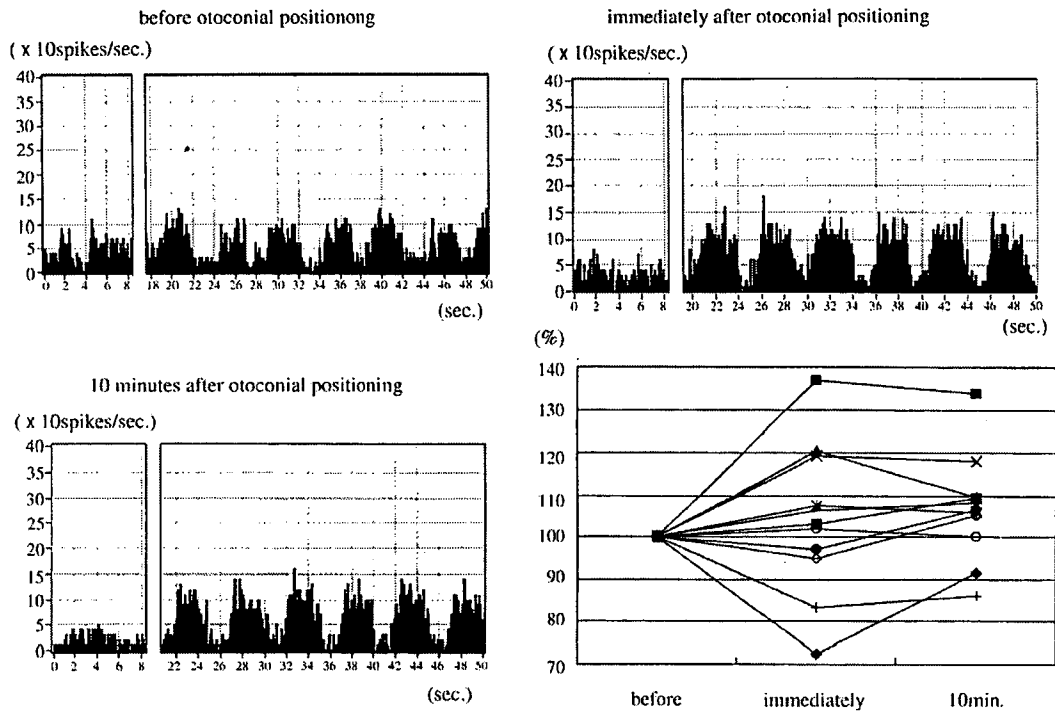


Fig. 5. Effect of positioned otoconial mass on the utricle with sinusoidal rotation (Experiment I-b (2)). Immediately after otoconial positioning the CAPs increased. It remained unchanged 10 min later. Changes in CAPs after the otoconial positioning are also graphically presented with the spike count before positioning as 100%. They increased in seven specimens and decreased in four.

3.3. Experiment II

The histograms of PSC CAPs in response to sinusoidal rotation showed sinusoidal oscillation of 0.1 Hz. In the normal specimen, the averaged response intensity was 245.9 spikes/s. In three out of eight canalolithiasis models it ranged from 200 spikes/s to 316.7 spikes/s. However, in another five specimens it markedly decreased. In four, the sinusoidal oscillation disappeared, leaving only spontaneous discharges. In the cupulolithiasis models the response intensity decreased in all specimens. In four specimens, the sinusoidal oscillation disappeared, leaving only spontaneous discharges (Fig. 6). Changes in the response intensity were expressed in percentage with the normal value as 100% (graphs in Fig. 6).

4. Discussion

Classical BPPV exhibits alternating rotatory nystagmus upon change of head-position. The theory of posterior canalolithiasis is widely accepted and head-positioning maneuvers are effective for quick resolution of vertigo [5,6]. Moreover, Suzuki et al. reported otoconial movement within the PSC and the CAP changes associated with otoconial movement in canalolithiasis model [4].

In a clinical setting patients often experience temporary vertigo or dizziness after physical therapy. Some patients even fall. It is suspected that the returned otoconia from PSC

irritate the utricular macula. However, this effect had never been investigated.

The kinocilium of the utricular macula is set into pores of the otoconial membrane on which the otoconia are densely distributed. In Experiment I-a, the CAPs in response to sinusoidal rotation disappeared when the otoconia were removed from the utricular macula. This suggests that the otoconia play an essential role as a transducer of acceleration. Suzuki et al. reported that the CAPs almost completely disappeared when the cupula was removed, but the CAPs resumed when it was replaced on the crista [3]. The otoconia has a physiological role analogous to the cupula.

The increase in utricular potentials observed immediately after positioning the otoconial mass in Experiment I-b (1) is possibly due to a direct effect of the otoconia on the sensory cells. This may well be a cause of the falls immediately after physical therapy.

Both centrifugal and tangential accelerations act upon a sinusoidal eccentric rotation. According to Koizuka [7] who quantified centrifugal and tangential accelerations in eccentric rotation, the centrifugal acceleration mainly acts for lower frequencies and the tangential acceleration mainly acts for higher frequencies over 0.64 Hz. The present experiment utilizes a low frequency of 0.1 Hz which exerts more centrifugal acceleration. Furthermore, in our experiment the effect of the tangential acceleration toward each direction of the sinusoid would be the same since this

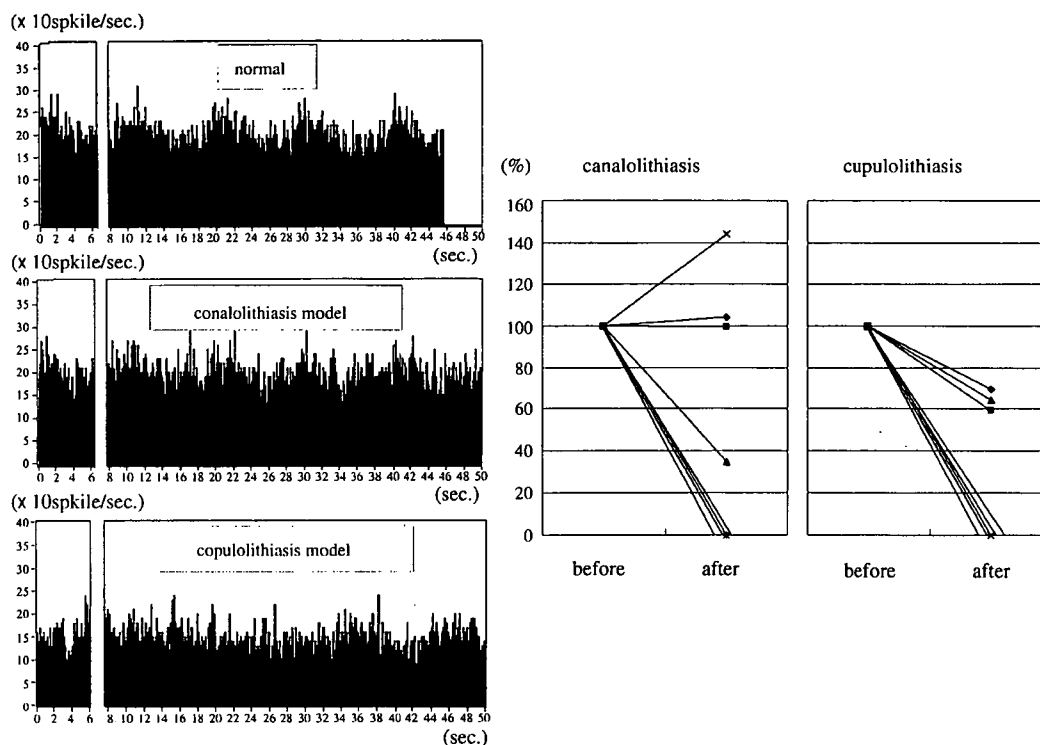


Fig. 6. Examples of CAP changes in canalolithiasis and cupulolithiasis models (Experiment II). The histograms in response to sinusoidal rotation yielded sinusoidal oscillation of 0.1 Hz. In three out of eight canalolithiasis models, the CAPs did not change or even increased. However, in another five specimens it markedly decreased or even disappeared (left graph). In the cupulolithiasis model, the CAPs were always inhibited. In three out of eight specimens, the CAPs were 60–70%, and in another five specimens the CAPs disappeared (right graph).

acceleration is along the main line of the striola. From these reasons, the effect of the centrifugal acceleration would be greater in the present experiment, thus resulting in the sinusoidal discharge (CAP).

The utricular CAPs due to rotatory stimulus increased in some specimens, but decreased in others after placing the otoconial mass in Experiment I-b (2). In view of the results of Experiment I-a, it was expected that the CAPs of all specimens in Experiment I-b (2) would increase after positioning the otoconial mass. Different CAP pattern is possibly due to the morphological polarity of the macular sensory cells. The sensory cells are divided with the striola into two groups. Whether the CAPs in response to sinusoidal rotation increase or decrease depends on the location of the positioned otoconial mass and the direction which the otoconial mass depresses the whole sensory cells, i.e., excitatory or inhibitory direction. Since the striola is located laterally, there are more cells in the medial portion. When the positioned otoconial mass depresses the kinocilia laterally, the centrifugal acceleration induces more CAP firing. Conversely, when the otoconial mass depresses them medially, the acceleration induces less firing. In any event, the CAPs change as a result of the otoconial positioning thus contributing to the temporary dizziness after physical therapy (Fig. 7). Shirane observed similar CAP changes in the magnetically stimulated utricle [8].

There are also reports that the caloric response reduces in BPPV patients [9,10]. While Sekine et al. [11] reported that there is no difference in the posterior canal VOR between normal and BPPV subjects. Our canalolithiasis model showed various changes of posterior canal CAP. In five specimens the CAP markedly decreased and even disappeared. The otoconia possibly formed an embolus thus blocking the endolymphatic flow. Possibility of otoconial debris forming an embolus was reported as canalith jam by Epley [12]. However, in three specimens of canalolithiasis models, the CAPs did not change or even increased. In these cases, the otoconia possibly moved with the endolymphatic flow, thus contributing to the increase in CAP. It is also easy to assume that CAP will be affected by the amount of otoconial mass within the canal. When the otoconial mass is small, CAP change will be further smaller. Sekine's cases are possibly with smaller canalolithiasis. The CAPs were inhibited in all specimens in cupulolithiasis models. This suppression of the CAPs is possibly due to the otoconial weight simply blocking the cupular displacement. This finding supports the clinical results that caloric response and VOR are more suppressed in cupulolithiasis than in canalolithiasis BPPV [13].

Our experiments suggest that reduced vestibular response does not necessary mean damage of the sensory cell function, but rather means inhibition of the cupular dynamics. This is supported by the clinical observation

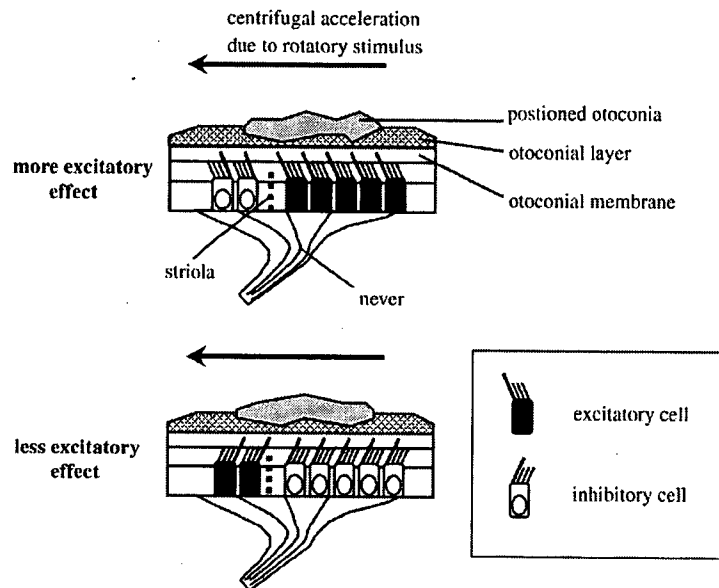


Fig. 7. Behavior of the positioned otoconial mass on the utricular macula. When the positioned otoconial mass depresses the cilia laterally, rotatory stimulus yields more excitation (upper figure). When it depresses them medially, less excitation occurs (lower figure).

that vertiginous spells rapidly resolve when an adequate physical therapy is performed. The imbalance of cupular mobility between normal and cupulolithiasis ears may be another cause of dizziness in BPPV patients.

5. Conclusion

Isolated utricles were used to investigate the mechanism of dizziness after physical therapy. Isolated PSC was used as canalolithiasis and cupulolithiasis models to investigate the mechanism of reduced VOR and caloric response.

The otoconia played an essential role as a transducer of acceleration to the utricular macula. Otoconial mass returned to the utricular macula appears to be the cause of dizziness after physical therapy. PSC responses to sinusoidal rotation were suppressed in cupulolithiasis model.

References

- [1] Hall SF, Ruby RRF, McClure JA. The mechanics of benign paroxysmal vertigo. *J Otolaryngol* 1979;8:151–8.
- [2] Suzuki M, Harada Y, Hirakawa H, Hirakawa K, Omura R. An experimental study demonstrating the physiological polarity of the frog's utricle. *Arch Otorhinolaryngol* 1987;244:215–7.
- [3] Suzuki M, Harada Y, Sugata Y. An experimental study on a function of the cupula: effect of cupula removal on the ampullary nerve action potential. *Arch Otorhinolaryngol* 1984;241:75–81.
- [4] Suzuki M, Kadir A, Hayashi N. Functional model of benign paroxysmal positional vertigo using an isolated frog semicircular canal. *J Vestib Res* 1996;6:121–5.
- [5] Epley JM. Positional vertigo related to semicircular canalolithiasis. *Otolaryngol Head Neck Surg* 1995;112:154–61.
- [6] Brandt T, Stedden S. Current view of the mechanism of benign paroxysmal positioning vertigo: cupulolithiasis or canalolithiasis? *J Vestib Res* 1993;3:373–82.
- [7] Koizuka I, Takeda N, Ogino H, Kubo T, Matsunaga T. Centric and eccentric pendular rotation test by use of MVM-C2. *Equilib Res* 1989;4:63–7.
- [8] Shirane M. Action potential from isolated frog utricle. *Equilib Res* 1983;42:16–20.
- [9] Baloh RW, Honrubia V, Jacobson K. Benign positional vertigo: clinical and oculographic features in 240 cases. *Neurology* 1987;37:371–8.
- [10] Korres SG, Balatsouras DG, Ferekidis E. Electronystagmographic findings in benign paroxysmal positional vertigo. *Ann Otol Rhinol Laryngol* 2004;113:313–8.
- [11] Sekine K, Imai T, Nakamae K, Morita M, Nakamae K, Miura K, et al. Vertical canal function in normal subjects and patients with benign paroxysmal positional vertigo. *Acta Otolaryngol* 2004;124:1046–52.
- [12] Epley JM. Caveats in particle repositioning fortreatment of canalithiasis (BPPV). *Head Neck Surg* 1997;8:68–76.
- [13] Sekine K, Imai T, Nakamae K, Fujioka H, Takeda N. Dynamics of the vestibulo-ocular reflex in patients with the horizontal semicircular canal variant of benign paroxysmal positional vertigo. *Acta Otolaryngol* 2004;124:587–94.

外側半規管型良性発作性頭位めまい症の臨床的検討

小川 恭生・鈴木 衛・市村 彰英
 萩原 晃・北島 尚治・稲垣 太郎
 湯川久美子・清水 重敬・竹之内 剛

Clinical Features of Benign Paroxysmal Positional Vertigo of the Horizontal Canal

Yasuo Ogawa, Mamoru Suzuki, Akihide Ichimura,
 Akira Hagiwara, Naoharu Kitajima, Taro Inagaki,
 Kumiko Yukawa, Sigetaka Shimizu and Tsuyoshi Takenouchi

(Tokyo medical university)

It has been considered that both ageotropic and geotropic direction-changing nystagmus frequently arise from central lesions, but lately, reports showing that direction-changing positional nystagmus is induced by peripheral lesions have increased. This study was designed to investigate the clinical features of horizontal canal variants of paroxysmal positional vertigo (HC-PPV). A retrospective study of 151 patients with HC-PPV was done. Patients complained of positional vertigo associated with direction-changing horizontal positional nystagmus, and either geotropic or ageotropic were examined. Horizontal nystagmus was triggered in all patients when rolled to either side in a supine position. The patients were 44 men and 107 women ranging from 24 to 88 years old (average 58.2 years old). The nystagmus was geotropic in 75 and ageotropic in 76 patients. There were many cases without latency in ageotropic cases, whereas there was latency in geotropic cases. As for the duration of the nystagmus, many ageotropic cases lasted more than one minute, whereas in many geotropic cases, the duration of nystagmus was less than one minute. Pure horizontal nystagmus was observed in most ageotropic cases, but in most geotropic cases, horizontal nystagmus with a torsional component was observed. Autotherapy was given to both geotropic and ageotropic cases. Geotropic cases tended to be cured in a short period compared with ageotropic cases, but some cases needed a longer time to cure in both groups. The "barbecue rotation" maneuver for treatment was performed in some cases. The effect of this maneuver was not so good as the Epley maneuver for BPPV.

Key words : BPPV, lateral semicircular canal, horizontal semicircular canal, apogeotropic, geotropic

はじめに

良性発作性頭位めまい症 (benign paroxysmal positional vertigo ; 以後 BPPV) は、主として耳石が半規管や膨大部に影響を及ぼして生じる内耳の機能異常である。BPPV のうち後半規管型 BPPV (posterior canal BPPV ; 以後 p-BPPV) は頻度が最も高く、その病態もよく知られ

ている。最近、頭位検査により方向交代性眼振を示し外側半規管に主に病巣があると想定される BPPV の報告が増加している^{1)~5)}。しかし p-BPPV とは異なり、外側半規管型 BPPV (lateral canal-BPPV ; 以後 l-BPPV) は眼振持続時間が長く、潜時のない症例もあり、その病態に関しては未だ不明の点が多い。また従来、方向交代性上向

性眼振は中枢性障害に多い⁶⁾とされており, 病因や病巣局在に関して議論がある⁷⁾. 今回, われわれはI-BPPV についてその臨床的特徴について検討した.

対象と方法

対象は1998年7月から2005年4月までの6年10ヵ月間に当科めまい外来を受診しためまい患者5156例の中の151症例である. これらは, 赤外線 CCD カメラ下に仰臥位6頭位で方向交代性上向性あるいは下向性頭位眼振を認めた. めまい感が強く, 脳神経学的所見がなく, 頭位眼振で垂直性眼振がなく, 視刺激検査で異常所見がなく, 中枢性病変を否定し, 他の末梢性疾患が否定され, 眼振の経時的变化を消失まで観察でき, BPPV と診断した症例である. 経過中一方向性(定方向)眼振がみられた症例や経過観察が不十分であった症例は除外した. めまい外来初診時の眼振の性状(水平性, 水平回旋混合性), 潜時の有無, 眼振の持続時間, 眼振消失までの期間について検討した. 眼振消失までの期間は, 方向交代性眼振を確認した日からめまい感, 眼振ともに消失した外来受診日までの期間とした.

結 果

対象症例の年齢は24歳から88歳で, 性別は男性44例(29.1%), 女性107例(70.9%)であった. 平均年齢は58.2歳であった. 全151例中方向交代性上向性眼振は76例, 方向交代性下向性眼振は75例であった(図1).

方向交代性上向性眼振症例76例の性別は, 男性26例, 女性50例であった(図1). 眼振の性状は水平性46例

(60.5%), 水平回旋混合性29例(38.2%), 水平斜行混合性1例(1.3%)であった(図2). 水平回旋混合性症例のうち5例に頭位変換検査で方向の逆転する回旋性眼振がみられ, p-BPPV の合併が示唆された. 眼振に潜時があった症例は19例, なかった症例は22例, その他35例はカルテに記載がなく不明であった(図3). 眼振の持続時間は1分以上続く症例が32例, 1分未満が15例, 不明が29例で, 1分以上持続する症例が多かった(図4). 経過中に眼振が変化した症例が22例あり, p-BPPV から方向交代性上向性眼振に変化した症例が5例, p-BPPV に変化した症例が6例, 方向交代性下向性眼振に変化した症例が7例あった.

当科を初診し, 方向交代性眼振確認後, 眼振消失までに要した日数は3日から1年以上とさまざまであった. 1週間以内に消失した症例が17例(22.4%), 8日以上1ヵ

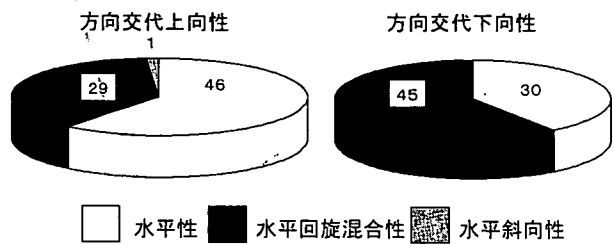


図2 眼振の性状

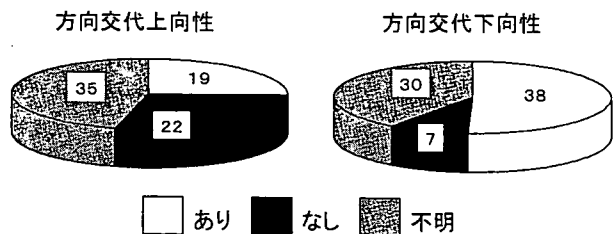


図3 眼振の潜時

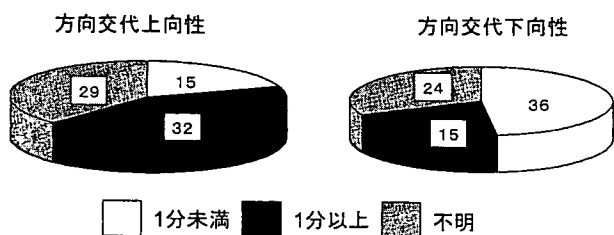


図4 眼振の持続時間

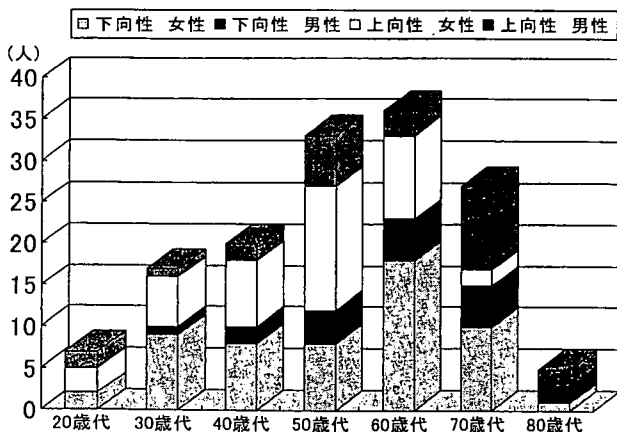


図1 年齢分布と性差

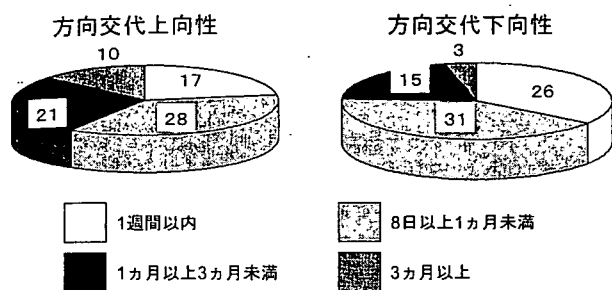


図5 眼振, めまい消失までの期間

月以内に消失した症例が28例(36.8%), 1~3ヵ月要した症例が21例(27.6%), 3ヵ月以上要した症例が10例(13.2%)であった(図5)。

方向交代性下向性眼振は75例あり, 性別は男性18例, 女性57例であった(図1)。眼振の方向は水平性30例(40.0%), 水平回旋混合性45例(60.0%)であった。水平回旋混合性症例のうち5例に頭位変換検査で方向の逆転する回旋性眼振がみられ, p-BPPVの合併が示唆された(図2)。眼振に潜時があった症例は38例, なかった症例は7例, 不明30例であった(図3)。眼振の持続時間は1分未満が36例, 1分以上が15例, 不明が24例であった(図4)。経過中に眼振が変化した症例が11例あり, p-BPPVから方向交代性上向性眼振に変化した症例が2例, p-BPPVに変化した症例が1例, 方向交代性上向性眼振に変化した症例が7例あった。

眼振消失期間は受診後3日から長期では6ヵ月以上に及んだ。1週間に以内に消失した症例は26例(34.7%), 8日から1ヵ月以内に消失した症例が31例(41.3%), 1から3ヵ月の間に消失した症例が15例(20.0%), 3ヵ月以上要した症例が3例(4.0%)であった(図5)。

16例に理学療法, barbecue rotation⁹⁾を行った。1回で治癒した症例が8例(50.0%), 2回で治癒した症例が1例, 繰り返して行ったが眼振, めまいが消失しなかった症例が4例(25.0%)あった。その他の3例は3回理学療法を施行し, 徐々に眼振, めまいが消失した。

次に症例を提示する。

症例1: 61歳, 女性。

主訴: 頭位変換時のめまい。

既往歴: 原発性胆汁性肝硬変, 食道静脈瘤で当院内科通院加療中。

現病歴: 2001年12月18日より頭位変換時のめまいが出現した。めまいは左右の側臥位, とくに左下頭位で著

明であった。12月25日当科めまい外来を受診した。

検査所見: 耳鼻咽喉頭に異常なく, 聴力検査も正常であった。X線で内耳道に左右差はなかった。蝸牛症状や脳神経症状, 小脳症状は認めなかった。

注視眼振検査で眼振はなかった。頭位眼振検査では, 右下頭位で左向き水平性眼振, 左下頭位で右向き水平性眼振を認めた。めまい感は左下頭位の方が強く, 眼振持続時間も左下の方が長く3分以上持続した。その後外来で経過をみていたがめまい症状と方向交代性上向性眼振は続いていた。1月24日に施行した視標追跡検査, 視運動性眼振には異常はなかった。頭位検査では, 方向交代性上向性眼振がみられた。左下頭位の方が眼振持続時間は長く, 頻度も高かった。2度目に頭位検査を行ったところ, 方向交代性下向性眼振に変わっていた(図6)。クプラに付着していた耳石が半規管内に落下し半規管結石症に移行したと考え barbecue rotation を行った。1月29日の頭位検査では再び方向交代性上向性眼振となっていた。眼振は微小で, めまい感はなかった。2月12日の再診時眼振は消失していた。

症例2: 70歳, 男性。

主訴: 頭位変換時のめまい。

既往歴: 急性骨髄性白血病で入院中。

現病歴: 2002年2月18日早朝, 坐位で上を向いたところ, 回転性めまいが出現した。同日当科外来を受診した。

検査所見: 耳鼻咽喉頭に異常なく, 聴力も正常であった。X線で内耳道に左右差はなかった。蝸牛症状や他の脳神経症状, 小脳症状は認めなかった。注視眼振はなかった。頭位眼振検査では右下頭位で左向き水平回旋混合性眼振, 左下頭位で右向き水平回旋混合性眼振を認めた。めまい感は右下頭位の方が強く, 潜時があり, 両側とも1分以内に眼振は消失した。再度確認のため頭位検査を行ったところ, 右下頭位で右向き, 左下頭位では左向きの水平回旋混合性眼振, すなわち方向交代性下向性眼振となっていた。2月26日当院再診時, 眼振は消失していた。

考 察

外側半規管に主病巣があると想定される BPPV には, 方向交代性上向性眼振と方向交代性下向性眼振を示すものがある。従来, 方向交代性頭位眼振は中枢疾患, とくにテント下疾患に多いとされていた。椎骨脳底動脈循環不全, 小脳脳幹梗塞, 第4脳室周囲の腫瘍などで上向性

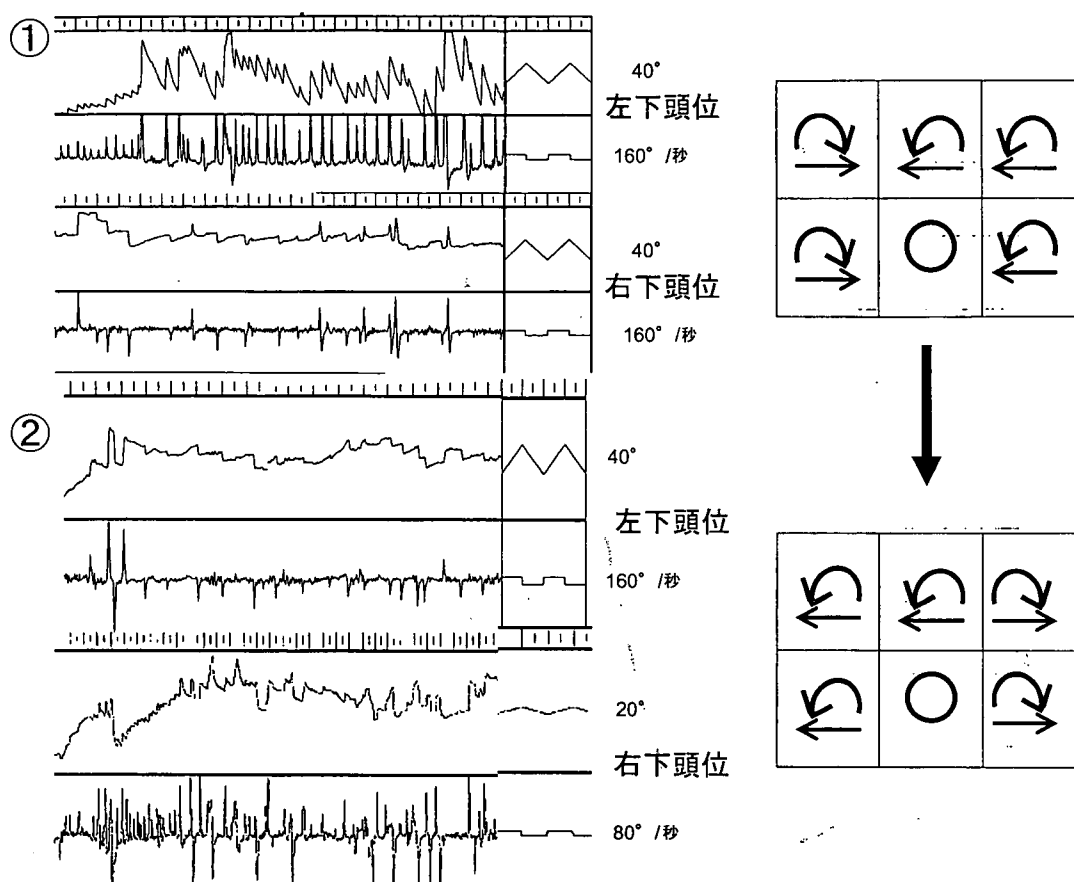


図 6 症例 1 頭位眼振図

- ①左下頭位で右向き, 右下頭位で左向きの眼振がみられた。
- ②再度頭位検査を行ったところ, 左下頭位で左向き, 右下頭位で右向きの眼振がみられた。

および下向性眼振が認められたとの報告が多く, 前庭神経核や片葉小節の障害が眼振の発現に関与すると考えられていた。しかし 1985 年の McClure⁹⁾ の報告や Pagnini ら¹⁰⁾, Baloh ら¹¹⁾ の報告以後, 方向交代性頭位眼振は中枢神経障害よりむしろ外側半規管に生じた BPPV によるものが多いと考えられるようになった。

①性差・好発年齢

好発年齢は過去の p-BPPV の報告と同様に, 50 歳から 60 歳代にピークがあった。Nuti ら¹⁾ の l-BPPV 123 症例の報告では, 年齢は 25 歳から 88 歳で平均は 55 歳と, 今回の結果と同様であった。性差は p-BPPV 同様, 女性に多いとされ¹²⁾, 今回の検討でも同様で, 耳石代謝とカルシウム代謝の関連が推察された¹³⁾。また 20 歳代から 60 歳代までは女性の割合が高いが, 70 歳代, 80 歳代では男性の割合が高くなっており, 高齢者の発症原因に耳石や

カルシウム代謝以外の加齢による要因¹⁴⁾が加わることが考えられた。

②眼振の成因

一般に方向交代性上向性眼振の成因は, 外側半規管のクプラに耳石や他の debris が付着したクプラ結石症とされている。患側上頭位をとった時に, 耳石が付着したクプラは向膨大部方向に偏位し患側向きの眼振が解発され, 患側下頭位ではその逆になるとされる。頭位を維持する限り重力加速度が働くので, Suzuki ら¹⁵⁾ の実験にあるように眼振の持続は長いと考えられる。今回提示した症例 1 は潜時がなく, 眼振の持続時間は 3 分以上持続しクプラ結石症によって方向交代性上向性眼振が生じたと考えられた。症例 1 では眼振図記録中にクプラに付着していた耳石が半規管内に落下し, 半規管結石症に移行したと考えられた。方向交代上向性眼振症例の多くは眼振

に潜時はなく、持続は1分以上であった。このような症例以外に症例2のように、方向交代性上向性眼振を示すが潜時を伴い眼振の持続が1分以内の症例もあった。一條ら¹⁶⁾は、クプラ結石症以外に外側半規管内に耳石が迷入し半規管の前方の部分で移動する場合と、膨大部の卵形囊側に耳石が迷入し膨大部内を移動する場合の2つの仮説を立てている。症例2は頭位検査を繰り返したところ眼振が方向交代性上向性から直ちに下向性に変化した。このことから、潜時を伴い眼振の持続時間が1分以内の方向交代性上向性眼振の原因は、クプラ結石症とするよりも、一條ら¹⁶⁾の仮説のように一種の半規管結石と考えられた。

方向交代性下向性眼振の成因は、半規管結石症と考えられている。患側下頭位で向膨大部性内リンパ流動が生じ、患側向きの眼振が解発され、健側下頭位では患側向きの眼振が解発される。多くの症例は眼振に潜時を伴い、持続は1分以内で減衰するものが多かった。一方、潜時のない症例や減衰がなく1分以上持続する症例もあり、眼振の発生機序として半規管結石症だけでは説明のつかない症例があった。

③眼振の性状

方向交代性下向性眼振症例では、水平性眼振に回旋成分が混在する症例の割合が高く、逆に方向交代性上向性眼振症例では純水平性眼振が多かった。回旋成分は、半規管結石症の場合後半規管にも同時に合併する可能性があることや¹⁷⁾、卵形囊障害に起因する眼振が混在するためと考えられている¹⁸⁾。半規管結石症が成因の場合、外側半規管の内リンパ流動のみでなく他の半規管、卵形囊にも内リンパ流動が波及するために回旋成分の混在が生じるが¹⁹⁾、クプラ結石症の場合、クプラの偏位は生じてもリンパ流動は半規管結石症ほど大きくなく、他の半規管や耳石器への影響が少なく回旋成分が混在しにくいと考えた。

④眼振消失までの期間

眼振消失までの期間は方向交代性上向性、下向性眼振症例どちらも1週間以内に消失する症例もあれば3ヵ月以上眼振が持続する症例もあり、眼振消失までの期間はさまざまであった。多くは、経過観察のみで自然に改善したが、一方で1年近く眼振が持続し半規管遮断術を施行した症例もあった²⁰⁾²¹⁾。方向交代性上向性症例は眼振、めまい感消失までに要した期間が1ヵ月未満59%、1ヵ月以上が41.0%と下向性症例に比べ長かった。眼振の変化

と治癒までの期間をみると次のような傾向がみられた。①方向交代性上向性眼振から変化することなく眼振、めまいとも速やかに消失する。②呈示した症例2のように検査中などに眼振が上向性から下向性に変化し比較的早く眼振、めまいが消失する。③方向交代性上向性眼振からしばらく経過して下向性に変化し消失する。④眼振の方向が変化せず、眼振、めまいが長期持続し徐々にめまい感、眼振とも消失する。①、②群は比較的早期に眼振、めまいが消失するが、③、④群の多くは眼振が1ヵ月から3ヵ月以上持続した。

方向交代性下向性症例は、方向交代性上向性眼振に比べ早期に眼振、めまい感とも消失する症例が多かった。方向交代性下向性眼振症例の治癒過程は次のようであった。①無治療のまま、早期に眼振、めまい感とも消失する。②理学療法にて眼振、めまい感とも消失する。③理学療法施行後もすぐに改善せず、徐々に眼振、めまい感が消失する。または無治療のまま徐々に眼振、めまい感が消失する。これら以外に改善までに1ヵ月以上要した症例の中にはp-BPPVの合併例、方向交代性上向性へ変化した例があり、眼振がさまざまに変化した症例で眼振、めまい感が長く残った。しかし方向交代性下向性眼振が変化しなかった症例においても眼振が長期持続するものがあつた。方向交代性上向性眼振、下向性眼振症例とも早期に自然治癒する過程はp-BPPVの自然治癒するものと比べ短い印象であった。

⑤理学療法

1-BPPVに対する治療法として、いくつかの理学療法の有効性が報告されている。今回の検討でも、方向交代性下向性眼振16症例にbarbecue rotationを試みた。Casaniら²²⁾は有効例が89.0%、無効例が11.0%としており、Nutiら²³⁾は有効66.7%、無効22.2%としている。今回の症例では、barbecue rotationを1回施行することにより眼振が消失した症例は50.0%で、25.0%の症例には無効であった。また理学療法有効例においても自然治癒の可能性は否定できない。治癒までの期間を短縮させた症例も有効例には入るが、p-BPPVに対する理学療法ほどの治癒率は得られない印象であった。

⑥方向交代性上向性眼振症例の患側

武田ら²⁴⁾、重野²⁵⁾は外側半規管クプラ結石症の患側決定について、強い眼振が誘発される頭位で上の耳が患側となり、この判定が困難な場合は、仰臥位正面で誘発される眼振が患側を向くことで判定できると述べている。

今回、方向交代性上向性眼振を呈しクプラ結石症と考えられ、頭位眼振に左右差があり、仰臥位正面で眼振がみられた15症例について検討した。強い眼振が誘発される頭位で上の耳が患側とした場合、仰臥位正面での眼振が患側向きであったのは10例、健側向きが5例であった。また上向性眼振症例でp-BPPVを合併、もしくは経過中にp-BPPVに変化し患側が推定可能であった症例を検討すると、仰臥位正面の眼振が10例中6例で患側向き、4例で健側向きであった。また、仰臥位正面で左向き眼振がみられた症例に右外側半規管遮断術を施行し眼振が消失した経験¹⁹⁾²⁰⁾もあり、仰臥位正面の眼振で患側を決定するのは今のところ困難と考えている。

⑦中枢性病変との鑑別

方向交代性頭位眼振の中枢性と末梢性の鑑別について、野村ら²⁶⁾はENG記録での眼振の性状から中枢性、末梢性を鑑別するのは困難と述べている。今回の検討でも、方向交代性上向性眼振症例、下向性眼振症例とも眼振の性状は多彩であった。また同一症例でも、初診時の激しい眼振がめまいを伴わない非常に弱い眼振に変化することも少なくなく、1回の眼振の観察のみで中枢と末梢を鑑別することは困難と思われた。近年の臨床検討^{1)~5)}や動物実験¹⁵⁾から方向交代性頭位眼振は中枢神経系の障害よりむしろ末梢前庭障害によることが多いと考えられるようになった。しかし方向交代性頭位眼振症例の診察では常に中枢障害を念頭に置くことは重要であり、糖尿病、高血圧、高脂血症といった循環障害をきたす基礎疾患の有無、他の神経症状の有無を確認し、眼振の経時的変化を観察すること、頭位変換検査で下眼瞼向き眼振の有無を確認することが重要である。

結 語

1. 頭位眼振検査で方向交代性眼振がみられ、l-BPPVと診断した方向交代性上向性眼振症例76例、下向性眼振症例75例について検討した。
2. 好発年齢は、50歳代から60歳代に多く、上向性眼振症例、下向性眼振症例とも女性が多かった。
3. 眼振の性状は方向交代性上向性では、純水平性眼振が多く、下向性症例では、水平性眼振に回旋成分が混在する症例が多かった。
4. 治癒までの期間は方向交代性上向性眼振症例の方が下向性眼振症例に比べて長く要する症例の割合が高かった。

5. 方向交代性上向性眼振症例、下向性眼振症例とも早期に自然治癒する症例もあったが眼振、めまい感が長期持続する症例が少なくなく、それら難治例の病態の把握、治療法の確立が必要と考えられる。

参考文献

- 1) Nuti D, Vannucchi P and Pagnini P : Benign paroxysmal positional vertigo of the horizontal canal: a form of canalolithiasis with variable clinical features. *J Vestib Res* 6 : 173 ~ 184, 1996.
- 2) De la Meilleure G, Dehaene I, Depondt M, et al. : Benign paroxysmal positional vertigo of the horizontal canal. *J Neurol Neurosurg Psychiatry* 60 : 68 ~ 71, 1996.
- 3) Bertholon P, Faye MB, Tringali S, et al. : Benign paroxysmal positional vertigo of the horizontal canal. Clinical features in 25 patients. *Ann Otolaryngol Chir Cervicofac* 119:73 ~ 80, 2002.
- 4) 高石 司 : 外側半規管型良性発作性頭位めまい症の臨床. *Equilibrium Res* 61 : 412 ~ 419, 2002.
- 5) 林裕次郎, 國弘幸伸, 東野一隆, 齋藤 昌, 神崎 仁 : 方向交代性頭位眼振の臨床的検討. *Equilibrium Res* 59 : 171 ~ 177, 2000.
- 6) 坂田英治 : 裸眼ないし Leuchtblille を用いた検査がめまい、平衡機能の診断に、どこまで助けとなりうるか. *耳鼻臨床* 63 : 431 ~ 463, 1970.
- 7) Yagi T, Morishita M, Kokawa M, et al. : Is the pathology of Horizontal canal benign paroxysmal positional vertigo really localized in the horizontal semicircular canal? *Acta Otolaryngol* 121 : 930 ~ 934, 2001.
- 8) Lempert T and Tiel-Wick K : A Positional maneuver for treatment of horizontal-canal benign positional vertigo. *Laryngoscope* 106 : 476 ~ 478, 1996.
- 9) McClure JA : Horizontal canal BPV. *J Otolaryngol* 14:30~35, 1985.
- 10) Pagnini P, Nuti D and Vannucchi P : Benign paroxysmal vertigo of the horizontal canal. *ORL J Otorhinolaryngol Relat Spec* 51 : 161 ~ 170, 1989.
- 11) Baloh RW, Jacobson K and Honrubia V : Horizontal semicircular canal variant of benign positional vertigo. *Neurology* 43 : 2542 ~ 2549, 1993.
- 12) Thomas Brandt : 頭位性および頭位変換性めまい. *めまい*. 262 ~ 273 頁, 診断と治療社, 東京, 2003.
- 13) Ross MD : Calcium ion uptake and exchange in otoconia. *Adv Otorhinolaryngol* 25 : 26 ~ 33, 1979.
- 14) Takumida M and Zhang DM : Electron probe X-ray microanalysis of otoconia in guinea pig inner ear. *Acta Otolaryngol* 117 : 529 ~ 537, 1997.
- 15) Suzuki M, Kadir A, Hayashi N, et al. : Functional model of

- benign paroxysmal positional vertigo using an isolated frog semicircular canal. *J Vestib Res* 6 : 121 ~ 125, 1996.
- 16) 一條宏明, 秋田二郎, 石井賢治, 宮腰靖始, 新川秀一 : 末梢性頭位眼振の種々の変化. *Equilibrium Res* 55 : 387 ~ 394, 1996.
- 17) Suzuki M, Yukawa K, Horiguchi S, et al. : Clinical feature of paroxysmal positional vertigo presenting combined lesions. *Acta Otolaryngol* 119 : 117 ~ 120, 1999.
- 18) 市村彰英, 鈴木 衛, 堀口利之, 北島尚治 : 方向交代性頭位眼振症例の検討. *Equilibrium Res* 62 : 88 ~ 95, 2003.
- 19) 平川治男, 鈴木 衛, 青木正則, 原田康夫 : 前庭受容器における 3 次元的相互作用—前半規管と後半規管—. *耳鼻臨床* 88 : 781 ~ 788, 1995.
- 20) Suzuki M, Ichimura A, Ueda K, et al. : Clinical effect of canal plugging on paroxymal positional vertigo. *J Laryngology Otol* 114 : 959 ~ 962, 2000.
- 21) 鈴木 衛 : 方向交代性頭位眼振の臨床. *耳鼻臨床* 93 : 177 ~ 183, 2000.
- 22) Casani AP, Vannucci G, Fattori B, et al. : The treatment of horizontal canal positional vertigo: our experience in 66 cases. *Laryngoscope* 112 : 172 ~ 178, 2002.
- 23) Nuti D, Agus G, Barbieri MT, et al. : The management of horizontal-canal paroxysmal positional vertigo. *Acta Otolaryngol* 118 : 455 ~ 460, 1998.
- 24) 武田憲昭 : 良性発作性頭位めまい症—臨床疫学と病態生理—. *耳鼻臨床* 94 : 763 ~ 776, 2001.
- 25) 重野浩一郎 : 外側半規管のクプラ結石症とクプラの位置. *Equilibrium Res* 61 : 97 ~ 98, 2002.
- 26) 野村公寿, 川西由美子, 内藤 明 : ENG における方向交代性頭位眼振の検討. *耳鼻咽喉* 52 : 935 ~ 941, 1980.

原稿受付 : 平成18年2月27日
 原稿採択 : 平成18年5月19日
 別刷請求先 : 小川恭生
 〒160-0023 東京都新宿区西新宿6-7-1
 東京医科大学耳鼻咽喉科学教室

Rapid-prototyped temporal bone and inner-ear models replicated by adjusting computed tomography thresholds

M SUZUKI, A HAGIWARA, Y OGAWA, H ONO*

Abstract

Purpose: This study aimed to investigate the validity of adjusting computed tomography thresholds in order to replicate a temporal bone model suitable for dissection training and education.

Materials and methods: A simulated three-dimensional model of a human temporal bone was prototyped using selective laser sintering. The powder layers were laser-fused, based on detailed computed tomography data, and accumulated to create a three-dimensional structure. The computed tomography threshold value of the stapes was modified on standard triangular language file in order to replicate the stapes. The intensity value was determined to select the fluid lumen of the inner ear and the bone surface, in order to replicate the inner ear.

Results: The model could be shaved, using surgical instruments, in the same manner as during real surgery. The stapes could be reproduced, making this model even more realistic than a previous version. The inner ear was recreated, along with the surrounding bony wall and the ossicles.

Conclusion: This model facilitates dissection training and easy understanding of the relation between the labyrinth and the surrounding structures.

Key words: Temporal Bone; Inner Ear; Model; Simulation; Computed Tomography

Introduction

The anatomy of the temporal bone is extremely complicated. Intensive training is required before the surgeon can master tympanoplasty. We previously created a three-dimensional (3D) model using a selective laser sintering method and reported its validity in surgical training and medical education.^{1–3} In the previous model, however, the stapes could not be reproduced because of its low radiopacity on computed tomography (CT) scanning. In this study, we attempted to replicate the stapes by enhancing its CT intensity.

The inner-ear model was made by simply reversing the CT value for bone replication.² This method eliminates data on the bone structure, and hence the model lacks the ossicles and the bony wall that covers the inner ear. In this study, we attempted to create both the inner ear and its surrounding bony structure by selecting both fluid and bone surface intensities.

Material and methods

The methods used to construct the temporal bone model have been reported in detail previously.¹ The derived 3D data were converted into the STL (standard triangular language) file. In order to

create the stapes, the CT intensity of the stapes was enhanced by changing the threshold value (Figure 1). When the intensity value of the bone part was simply reversed, the inner-ear part, as well as all the air space, was created.² In the present study, the intensity value was adjusted so that both the bony part and the air space were eliminated, but the area with an intensity between that of bone and the air, such as the fluid or the bone surface, could be retained (Figure 2). The derived 3D data were converted into a STL file system.

The powder material, polyamide nylon plus glass beads, was laser sintered according to the STL protocol. The created model was dissected using conventional otosurgical instruments.

Results

The appearance of the replicated stapes is shown in Figure 3. The posterior canal wall was removed. The malleus, incus and posterior crus of the stapes could be seen. Other structures, such as the mastoid air cells, surgical dome, facial nerve, promontory, auditory tube, round window niche, semicircular canal and cochlea, were recreated as in the previous model.¹ Figure 4 shows the replicated stapes seen from the external canal side after removing other

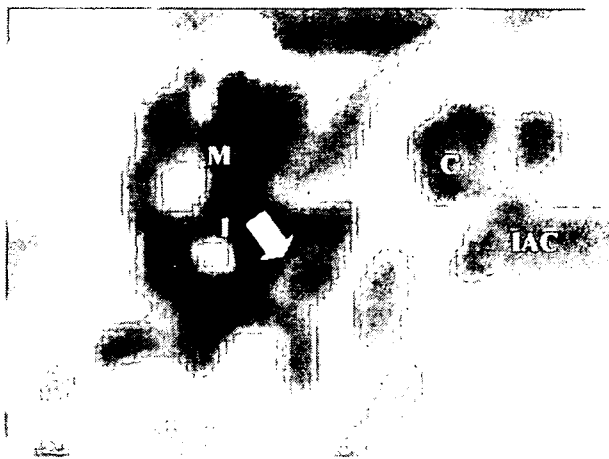


FIG. 1

Axial computed tomography showing the ossicles. The malleus (M) and the incus (I) are radiopaque, but the stapes (arrow) is far less so. The intensity value of the stapes was enhanced along each slice. C = cochlea; IAC = internal auditory canal

ossicles. The neighboring structures, such as the facial nerve, pyramidal eminence and promontory, are demonstrated. Another stapes model is shown in Figure 5 after removing the posterior canal and incus. In this case, the stapes head and two arches can easily be identified.

The whole appearance of the inner-ear model, replicated as per the previously published method,² is shown in Figure 6. In this model, the inner-ear parts as well as the air space were replicated, as only the radiopaque bony area was eliminated. The inner ear and the compact external ear canal were shown, but no ossicles were reproduced. In the present model, the inner ear, as well as the

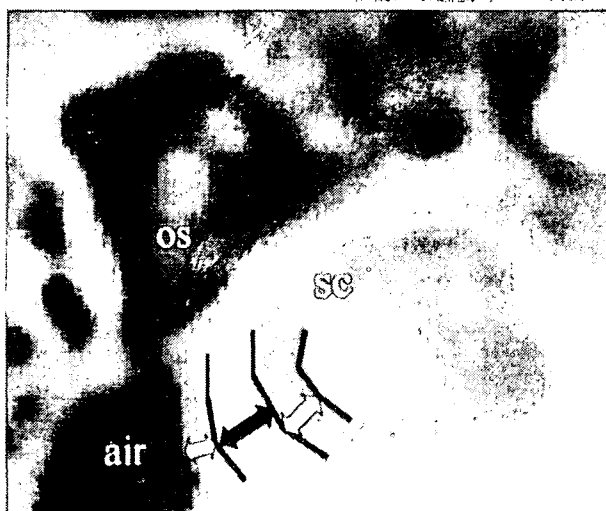


FIG. 2

Determination of the computed tomography value on STL data. The most radiopaque bone area (black arrow) and the air were eliminated. The intensity of the fluid and the bone surface (white arrows) was selected. OS = ossicle; SC = semi-circular canal

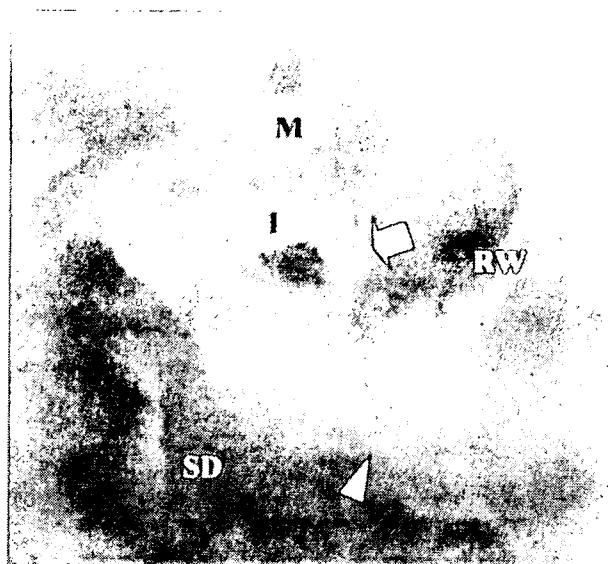


FIG. 3

Replicated model of right ear stapes. The posterior canal wall is removed. The posterior crus and incudostapedial joint are seen (arrow). M = malleus; I = incus; RW = round window niche; SD = surgical dome; arrow head = facial nerve

surrounding bony wall and the ossicles were created, since both the radiopaque bone area and the lucent air space were eliminated (Figure 7). The auditor canal wall, promontory, window niches, malleus, incus, stapes, facial nerve, surgical dome, and epitympanic tegmen were reproduced. The inner ear, including semicircular canals, cochlea and endolymphatic sac, and the internal auditory meatus were also reproduced, as in the previous model. The present model allows easier demonstration of the labyrinth's anatomical relation to the

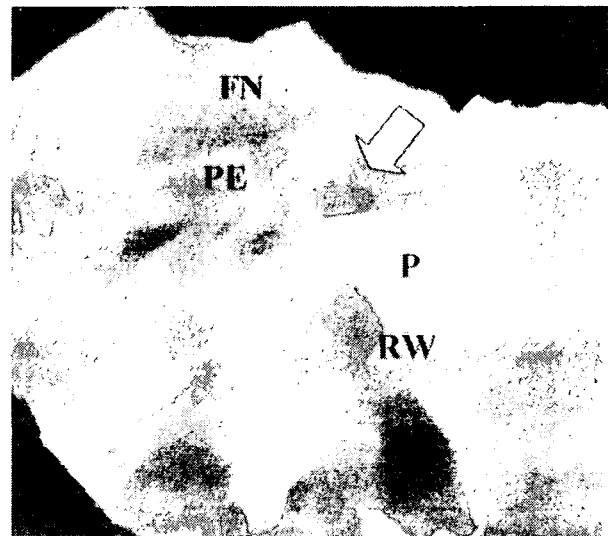


FIG. 4

Replicated stapes seen from the external canal. The superstructure of the stapes is shown (arrow). FN = facial nerve; PE = pyramidal eminence; P = promontory; RW = round window niche

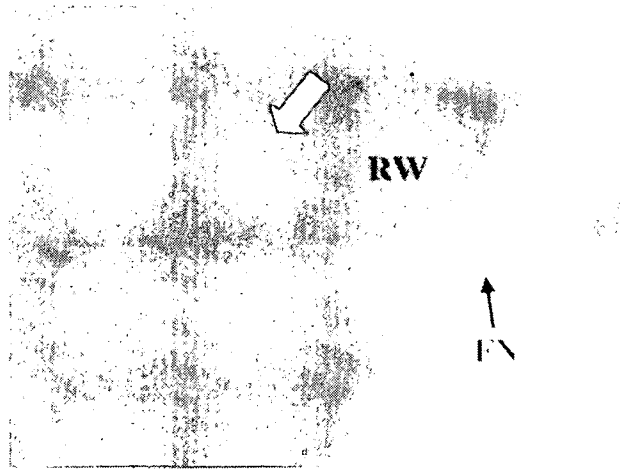


FIG. 5

Replicated stapes of another case, right ear. The posterior canal wall and the incus are removed. The crura and the head of the stapes are seen (arrow). RW = round window niche; FN = facial nerve

ossicles, surgical dome, promontory and window niches.

Discussion

It is not easy to acquire the skills required to perform tympanoplasty, because of the anatomical complexity of the ear. In recent years, computerised 3D displays of the temporal bone and 'virtual reality' endoscopic images have been developed.^{4,5} In cases with anatomical anomalies, safe surgery is extremely difficult, even after scrutinising the CT. Navigational

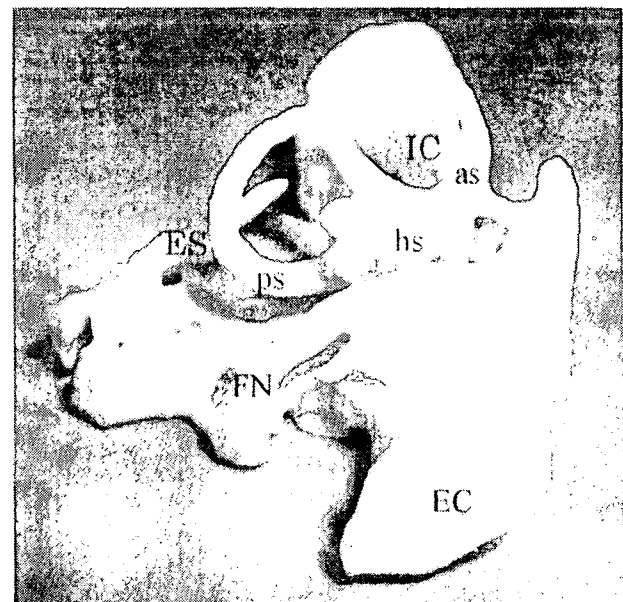
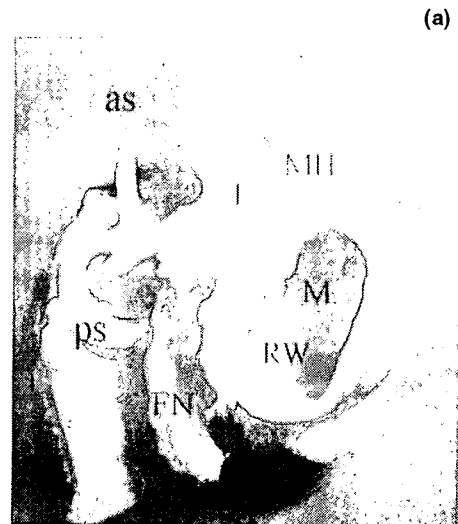
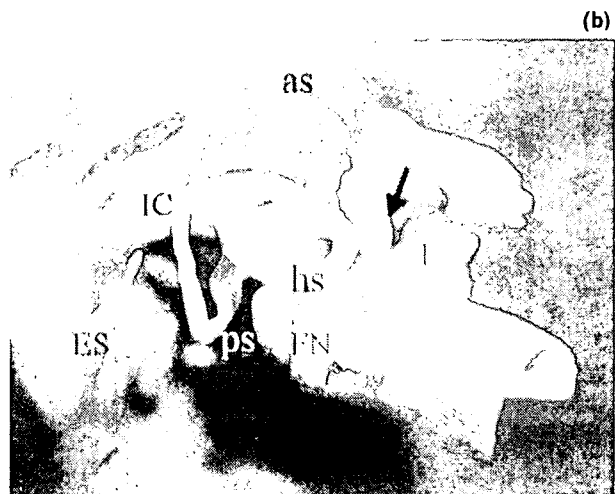


FIG. 6

Inner-ear model replicated using the previous method. Note the compact external canal (EC). No ossicles were created. IC = internal auditory canal; ES = endolymphatic sac; FN = facial nerve; as = anterior semicircular canal; hs = horizontal semicircular canal; ps = posterior semicircular canal



(a)



(b)

FIG. 7

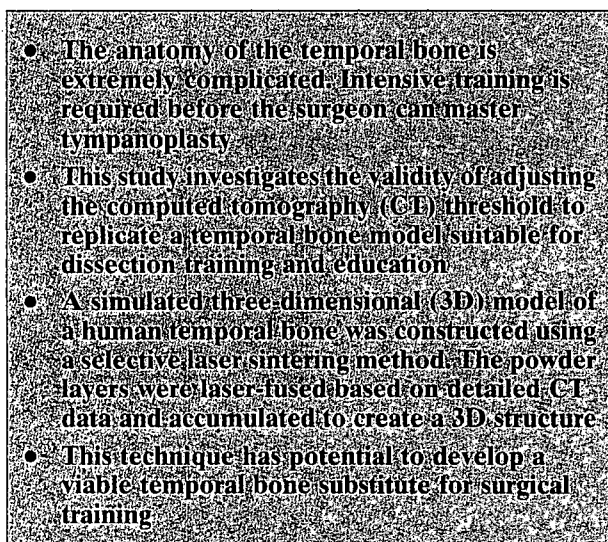
Inner-ear models replicated by the present method. (a) The contour of the external canal is recreated. The malleus, incus and round window niche (RW) can be seen through the canal. (b) In another model, the anatomical relationship between the semicircular canals and the incus, facial nerve and surgical dome (arrow) can be easily seen. The lower half of the external canal has been cut. IC = internal auditory canal; ES = endolymphatic sac; FN = facial nerve; MH = malleus head; I = incus; as = anterior semicircular canal; hs = horizontal semicircular canal; ps = posterior semicircular canal; M = malleus

surgery and robotic surgery allow good orientation of abnormal structures and ensure safety.^{6,7} However, these interventions are costly and require much space and equipment. Rapid prototyping is cost-effective and allows replication of anatomical details. In particular, the models created using selective laser sintering allow easy dissection and are particularly suited for pre-operative simulation.¹

In the previous model, the stapes could not be replicated because of its low density on STL data, as shown in Figure 1, although the malleus and incus could be reproduced. In this study, we attempted to locally enhance the stapes' radiopacity by changing the threshold value on STL data. This allowed replication of the stapes, including both

crura and head. The anatomical location of the stapes is extremely important, since it serves as a good landmark to locate other structures such as the horizontal segment of the facial nerve and the round window niche. The present model has more advantages as an educational resource, compared with the past model.

The inner-ear model serves as a good resource when teaching 3D orientation within the inner ear.² The structural features of the model, such as the internal auditory meatus, facial nerve and endolymphatic sac, allow easy understanding of the inner ear within its wider context. The model can be used as an anatomical guide while dissecting the temporal bone model. The present model is useful for teaching the relationship between the inner ear and the surrounding bone structure. There are clinically important landmarks around the labyrinth, such as the incus short process, surgical dome, promontory and window niches. The anatomical relations between the labyrinth and these structure can readily be demonstrated using this 3D model.



In the future, we will examine the extent to which medical trainees can develop their anatomical knowledge and surgical skills by using these models. We will also study replication of an ossicular anomaly, by adjusting the local threshold value of

deformed ossicles. Three-dimensional evaluation of congenitally malformed ears will also give us new insights into the developmental process of the ear.

Conclusion

Using the rapid-prototyping technique, the CT threshold was modified in order to replicate the stapes. The temporal bone model, with stapes intact, has great advantages as an educational resource. By adjusting the intensity value of the CT, the bony labyrinth and the surrounding bone structure could be recreated. The model contributes to easy understanding of the relationship between the labyrinth and the surrounding structures.

References

- 1 Suzuki M, Ogawa Y, Kawano A, Hagiwara A, Yamaguchi H, Ono H. Rapid prototyping of temporal bone for surgical training and medical education. *Acta Otolaryngol* 2004; **124**:400–2
- 2 Suzuki M, Ogawa Y, Hagiwara A, Yamaguchi H, Ono H. Rapid-prototyped temporal bone model for otological education. *ORL J Otorhinolaryngol Relat Spec* 2004; **66**:62–4
- 3 Suzuki M, Hagiwara A, Kawaguchi S, Ono H. Application of a rapid-prototyped temporal bone model for surgical planning. *Acta Otolaryngol* 2005; **125**:29–32
- 4 Morra A, Tirelli G, Rimondini A, Cioffi V, Russolo M, Giacomarra V, Pozzi-Mucelli R. Usefulness of virtual endoscopic three-dimensional reconstructions of the middle ear. *Acta Otolaryngol* 2002; **122**:382–5
- 5 Begall K, Vorwerk U. Artificial petrous bone produced by stereo lithography for microsurgical dissecting exercises. *ORL J Otorhinolaryngol Relat Spec* 1998; **60**:241–5
- 6 Selesnick SH, Kacker A. Image-guided surgical navigation in otology and neurotology. *Am J Otol* 1999; **20**:688–93
- 7 Federspil PA, Geithoff UW, Henrich D. Development of the first force-controlled robot for otoneurosurgery. *Laryngoscope* 2003; **113**:465–71

Address for correspondence:

Dr Mamoru Suzuki,
Department of Otolaryngology,
Tokyo Medical University,
6-7-1 Nishishinjuku,
Shinjuku-ku, Tokyo, Japan 160-0023.

Fax: +81 3 3346 9275

E-mail: otosuzu@tokyo-med.ac.jp

Dr M Suzuki takes responsibility for the integrity of the content of the paper.

Competing interests: None declared

ORIGINAL ARTICLE

Transient receptor potential channels in the inner ear: Presence of transient receptor potential channel subfamily 1 and 4 in the guinea pig inner ear

MASAYA TAKUMIDA¹, NOBUO KUBO², MAKIKO OHTANI², YUKO SUZUKA³ & MATTI ANNIKO⁴

Departments of Otolaryngology, ¹Hiroshima University Faculty of Medicine, Hiroshima, Japan, ²Kansai Medical University, Osaka, Japan and ³Kanazawa Medical University, Kanazawa, Japan, and the ⁴Department of Otolaryngology, Head and Neck Surgery, University Hospital, Uppsala, Sweden

Abstract

Conclusion. The results of this study indicate that transient receptor potential subfamily 1 (TRPV1) may play a functional role in sensory cell physiology and that TRPV4 may be important for fluid homeostasis in the inner ear. **Objective.** To analyze the expression of TRPV1 and -4 in the normal guinea pig inner ear. **Material and methods.** Albino guinea pigs were used. The location of TRPV1 and -4 in the inner ear, i.e. cochlea, vestibular end organs and endolymphatic sac, was investigated by means of immunohistochemistry. **Results.** Immunohistochemistry revealed the presence of TRPV1 in the hair cells and supporting cells of the organ of Corti, in spiral ganglion cells, sensory cells of the vestibular end organs and vestibular ganglion cells. TRPV4 was found in the hair cells and supporting cells of the organ of Corti, in marginal cells of the stria vascularis, spiral ganglion cells, sensory cells, transitional cells, dark cells in the vestibular end organs, vestibular ganglion cells and epithelial cells of the endolymphatic sac.

Keywords: Immunohistochemistry, inner ear, transient receptor potential channel subfamily 1 and 4

Introduction

The recent discovery of a new class of calcium-permeable cationic channels, the transient receptor potential (TRP) channel superfamily, has given major insights into the molecular entities and signaling mechanism controlling calcium influx into a broad range of cells [1,2]. TRP channels are widely expressed in both excitable and non-excitable cells of vertebrates and invertebrates, where they appear to act as primary pathways for regulated calcium entry.

The TRP family channels, of which >25 members have now been identified, have recently been classified into 3 main groups, with a fourth group under consideration. The subfamilies are: TRPC, the classical or conical-like TRP channels; TRPV, the vanilloid receptor-like channels; TRPM, the melastatin-like channels; and TRPP, the two protein-like channels implicated in polycystic kidney

disease. The functions of the TRP channels of the various subfamilies are only partly known but they appear to support a variety of functions, ranging from sensory transduction to secretion and proliferation [1,2].

Recently, the TRPV subfamily has attracted increasing attention because of the expanding role that some members of this group appear to play in both sensory and non-sensory transduction. In mammals, vanilloid-sensitive neurons can be excited by a variety of noxious agents, such as chemical, mechanical or thermal stimuli, that transmit nociceptive information from the periphery to the central nervous system (CNS), producing a sensation of burning pain. These neurons, called nociceptors, are characterized in part by their sensitivity to capsaicin, the pungent ingredient in “hot” chilli peppers [3,4]. Capsaicin exerts its effect on nociceptors by

Correspondence: Masaya Takumida, Department of Otolaryngology, Faculty of Medicine, Hiroshima University, 1-2-3 Kasumicho, Minamiku, Hiroshima 734-8551, Japan. E-mail: masati@ipc.hiroshima-u.ac.jp

(Received 6 April 2005; accepted 7 April 2005)

ISSN 0001-6489 print/ISSN 1651-2551 online © 2005 Taylor & Francis
DOI: 10.1080/00016480510038572